This article was downloaded by:
On: *25 January 2011*
Access details: *Access Details: Free Access*
Publisher *Taylor & Francis*
Informa Ltd Registered in England and Wales Registered Number: 1072954 Registered office: Mortimer House, 37-41 Mortimer Street, London W1T 3JH, UK

Liquid Crystals
Publication details, including instructions for authors and subscription information:
http://www.informaworld.com/smpp/title~content=t713926090

Mesomorphic behaviour and TSDC measurements of *ortho*-metallated palladium(II) and platinum(II) complexes with S,O-donor co-ligands

Viorel Cîrcu[a]; Doina Mănăilă-Maximean[b]; Constantin Roşu[b]; Monica Iliş[a]; Yann Molard[c]; Florea Dumitraşcu[d]
[a] Inorganic Chemistry Department, University of Bucharest, Bucharest, sector 2, Romania [b] Physics Department II, University "Politehnica Bucuresti", Bucharest, Romania [c] Sciences Chimiques de Rennes UMR 6226 CNRS Université de Rennes 1, Avenue du Général Leclerc, Rennes Cedex, France [d] Centre of Organic Chemistry "C.D. Nenitzescu", Romanian Academy, Bucharest, Romania

To cite this Article Cîrcu, Viorel , Mănăilă-Maximean, Doina , Roşu, Constantin , Iliş, Monica , Molard, Yann and Dumitraşcu, Florea(2009) 'Mesomorphic behaviour and TSDC measurements of *ortho*-metallated palladium(II) and platinum(II) complexes with S,O-donor co-ligands', Liquid Crystals, 36: 2, 123 — 132
To link to this Article: DOI: 10.1080/02678290802696173
URL: http://dx.doi.org/10.1080/02678290802696173

PLEASE SCROLL DOWN FOR ARTICLE

Full terms and conditions of use: http://www.informaworld.com/terms-and-conditions-of-access.pdf

This article may be used for research, teaching and private study purposes. Any substantial or systematic reproduction, re-distribution, re-selling, loan or sub-licensing, systematic supply or distribution in any form to anyone is expressly forbidden.

The publisher does not give any warranty express or implied or make any representation that the contents will be complete or accurate or up to date. The accuracy of any instructions, formulae and drug doses should be independently verified with primary sources. The publisher shall not be liable for any loss, actions, claims, proceedings, demand or costs or damages whatsoever or howsoever caused arising directly or indirectly in connection with or arising out of the use of this material.

Liquid Crystals,
Vol. 36, No. 2, February 2009, 123–132

Taylor & Francis
Taylor & Francis Group

Mesomorphic behaviour and TSDC measurements of *ortho*-metallated palladium(II) and platinum(II) complexes with S,O-donor co-ligands

Viorel Cîrcu[a]*, Doina Mănăilă-Maximean[b], Constantin Roşu[b], Monica Iliş[a], Yann Molard[c] and Florea Dumitraşcu[d]

[a]*Inorganic Chemistry Department, University of Bucharest, 23 Dumbrava Rosie st., 020464, Bucharest, sector 2, Romania;* [b]*Physics Department II, University "Politehnica Bucuresti", Splaiul Independentei 313, Bucharest 060042, Romania;* [c]*Sciences Chimiques de Rennes UMR 6226 CNRS Université de Rennes 1, Avenue du Général Leclerc 35042 Rennes Cedex, France;* [d]*Centre of Organic Chemistry "C.D. Nenitzescu", Romanian Academy, Splaiul Independentei 202B, Bucharest, 060023, Romania*

(Received 1 November 2008; final form 16 December 2008)

A series of *ortho*-metallated Pd and Pt complexes containing an imine ligand carrying three alkoxy chains and *N*-benzoylthiourea derivatives as co-ligands were prepared and their liquid crystalline properties investigated. Their structures were assigned based on elemental analysis, IR and ^{1}H NMR spectroscopy, whereas thermal properties were investigated by differential scanning calotimetry and polarising optical microscopy. All the compounds exhibit monotropic transitions involving nematic and smectic A phases, with the mesomorphic behaviour strongly related to the type of *N*-benzoylthiourea as well as the metal centre used. The thermally stimulated depolarisation current technique was employed to determine the conduction mechanism, phase transition temperature and the activation energies for one of the *ortho*-metallated Pd complexes.

Keywords: palladium complex; platinum complex; *ortho*-metallation; *N*-benzoylthiourea derivative; TSDC

Downloaded At: 14:54 25 January 2011

1. Introduction

Palladium and platinum organometallic complexes with nitrogen-containing heteroaromatic ligands represent one of the most interesting and intensively studied class of metallomesogens (metal-containing compounds displaying liquid crystalline behaviour), and consist of both dinuclear and mononuclear organometallic systems (*1*).

One of the most widely used class of heteroaromatic ligands is represented by the imine ligands that have been used in *ortho*-metallation reactions and have shown a strong tendency to form, with palladium and platinum precursors, cyclometallated five-membered rings containing the metal ions in a square-planar environment. In this way, a large number of di- and mononuclear species with liquid crystal properties has been prepared and investigated, due to the different possibilities for tuning the mesogenic properties of such compounds, as well as other physico-chemical properties (*2*).

On the other hand, in order to reduce the transition temperatures and to keep a broad mesomorphic range in such systems containing the *ortho*-metallated imine fragment, various co-ligands have been introduced, which lead, in most of the cases, but not always, to mononuclear compounds with more accessible and sometimes more stable mesophases compared with the dinuclear parent complexes. Several classes of co-ligands were used to prepare mononuclear species with improved mesogenic properties, e.g. β-diketones (*3*), β-aminoenonates (*3a*, *4*), α-amino acids (*5*), cyclopentadienyls (*6*) or dialkyldithiocarbamates (*7*). For example, it is well known that dimeric compounds $[(C\text{-}N)PdCl]_2$ (C-N = *ortho*-palladated imine with two long alkyl chains) form smectic A (SmA) and smectic C (SmC) phases at high temperatures, whereas the monomeric complexes with β-diketonate ligands [(C-N)Pd(acac)] form nematic and SmA phases at significantly lower temperatures (*3a–3c*).

In previous studies, we have shown that the use of *N*-benzoylthiourea derivatives as co-ligands in combination with the *ortho*-palladated imine fragment destabilises the mesogenic behaviour of these complexes and a monotropic nematic phase is observed (*8*). Indeed, these derivatives proved to be very good chelating ligands due to the presence of two very strong donor groups (carbonyl and thioamide), reacting with transition metals mostly in monoanionic and bidentate form by deprotonation, resulting in neutral complexes with S,O-coordination (*9*). Only few other studies (*10–12*) dealing with purely organic liquid crystals based on *N*-benzoylthiourea moiety have been reported previously, which prompted us to extend the study regarding the influence of *N*-benzoylthiourea derivatives on the mesogenic behaviour of *ortho*-metallated imine fragment in order to establish some structure–property correlations and to prepare liquid crystalline materials with low transition temperatures and broad mesomorphic range.

*Corresponding author. Email: viorel_carcu@yahoo.com

ISSN 0267-8292 print/ISSN 1366-5855 online
© 2009 Taylor & Francis
DOI: 10.1080/02678290802696173
http://www.informaworld.com

In this paper, we report the preparation, the mesogenic behaviour and thermally stimulated depolarisation current (TSDC) measurements of a series of *ortho*-metallated palladium and platinum complexes with an imine ligand carrying three alkoxy chains and having *N*-benzoylthiourea derivatives as co-ligands.

It was previously shown that the molecular geometry and the number of peripheral chains linked to the aromatic core of imine *ortho*-metallated mesogens greatly influence the type of mesophase exhibited in the case of dinuclear complexes. Thus, the first examples of both mono- and dinuclear palladium *ortho*-metallated complexes with imine ligands carrying three alkyl chains were reported recently to show SmA and SmC phases (*13*), whereas the related dinuclear compounds with imine ligands bearing four alkyl chains, due to their sheet-like shape, exhibit nematic discotic mesophases (*14*).

The TSDC method is a powerful tool for determination of phase transitions, which often present resolution difficulties with other techniques (*15*, *16*), activation energies and the nature of the conduction mechanism in a material. The TSDC spectra exhibit several peaks indicating different processes occurred in the sample (depolarisation of permanent dipoles, release of charges, polarisation changes connected to phase transitions), whereas the optical transmission is simultaneous.

Downloaded At: 14:54 25 January 2011

2. Results and discussion

The synthetic pathway used to prepare the palladium(II) and platinum (II) complexes is depicted in Scheme 1. The dinuclear acetato-bridged palladium complex **2** was obtained by *ortho*-palladation reaction of the imine **1**, by using $[Pd(OAc)_2]_3$, with good yield. The mononuclear Pd(II) complexes were prepared by reacting the dinuclear acetato-bridged complex with sodium salts of *N*-benzoylthiourea derivatives (NaBTU) in dichloromethane. These mononuclear complexes were obtained in moderate to good yields as yellow microcrystalline solid products, which are stable under atmospheric conditions. The dinuclear chloro-bridged *ortho*-platinated compound was prepared by *ortho*-platination of the imine ligand using $[Pt(\mu\text{-}Cl)(\eta^3\text{-}C_4H_7)]_2$ as starting material. The crude product was used in the next step for the preparation of the mononuclear species without further characterisation and purification. The preparation of mononuclear *ortho*-platinated complexes was carried out by ligand exchange reaction of the chloro-bridged dinuclear platinum(II) complex using the corresponding sodium salts of the *N*-benzoylthiourea derivatives. The new platinum(II) complexes were obtained in moderate yields as orange microcrystalline solid products.

All the new products were characterised by elemental analysis, IR, ^{1}H NMR spectroscopy whereas the liquid crystal properties were investigated by differential scanning calorimetry (DSC) and polarising optical microscopy (POM).

The formation of the mixed-ligands *ortho*-metallated mononuclear complexes can be confirmed readily by IR and ^{1}H-NMR spectroscopy when the coordination of the *N*-benzoylthiourea derivatives in the deprotonated form is confirmed by the disappearance of ν_{NH} ($\sim$3300 cm^{-1}) and $\nu_{C=O}$ ($\sim$1670 cm^{-1}) frequencies (compared to the IR spectra of free ligands) together with a shift of $\nu_{C\text{-}N}$ frequency towards lower wavenumbers. All this information suggests the absence of NH hydrogen located between carbonyl and thiocarbonyl groups of the benzoyl thioureic moiety, which is further supported by ^{1}H NMR spectroscopy.

The ^{1}H NMR spectra of platinum(II) complexes show the ^{195}Pt satellites, which confirm that the *ortho*-platination process occurred, and from which the coupling constants $^3J_{Pt\text{-}H}$ were deduced. The values of these constants were in the expected range for such compounds and are similar with those found for other *ortho*-platinated complexes (*17*).

Another interesting feature of the ^{1}H NMR spectra of mononuclear palladium and platinum(II) complexes is the presence of only one set of signals, which suggests the presence of only one isomer in solution, as was previously found in the case of *ortho*-metallated palladium(II) complexes containing an imine ligand with two alkoxy chains and *N*-benzoythiourea derivatives as co-ligands (it is possible for these complexes to exist as a mixture of two isomers, with the sulfur atom of the *N*-benzoylthiourea ligand in *trans* or *cis* position to the nitrogen atom of the azomethine group of the imine ligand) (*8*).

2.1 Thermal behaviour

The palladium and platinum complexes were investigated for their potential liquid crystal properties by a combination of hot-stage POM and DSC. The thermal data are presented in Table 1. The mesophases were assigned based on their optical texture, three examples of which are shown in Figures 1–2. It is worth noting that the imine with three alkoxy chains used as ligand is not a liquid crystal (**1**: Cr–I, 74°C).

Both palladium(II) and platinum(II) complexes exhibit a monotropic SmA phase, which could be assigned by the typical fan-shaped texture that can be aligned homeotropically. The complexes **5** and **6** exibit an additional monotropic nematic phase on

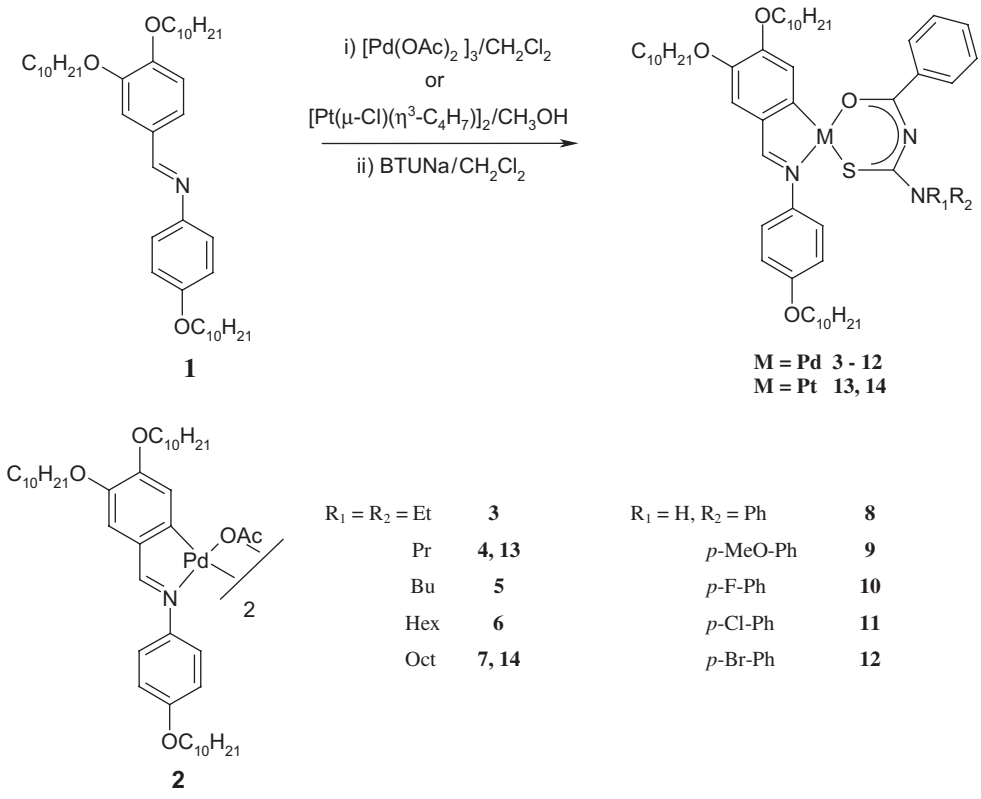

Scheme 1. Preparation of mononuclear Pd(II) and Pt(II) *ortho*-metallated complexes.

Downloaded At: 14:54 25 January 2011

cooling from the isotropic liquid, with typical schlieren and marbled textures (Figure 3).

The thermal behaviour of these complexes is not unexpected as they can be regarded as tricatenar systems for which the presence of smectic and nematic phases is well known. The only compound reported in the literature and available for comparison from this point of view is an *ortho*-metallated Pd(II) complex that posseses an imine ligand with three alkyl chains and a β-substituted-phenyldiketonate as co-ligand, which exhibits a monotropic nematic phase (*18*). Thus, it is clear that the use of *N*-benzoylthiourea derivatives as co-ligands together with the *ortho*-metallated imine fragment destabilises the mesogenic behaviour of these complexes to such an extent that only monotropic behaviour is seen for all prepared complexes, with the temperature of the transition to mesophase within a broad range 10–45°C below the clearing temperature, depending on the type of substituents of the benzoyl thioureic moiety. Interestingly, the smectic phase of Pd complexes is stable up to room temperature for several hours after which a slow crystallisation process occurs, whereas in the case of complex **3** several heating to isotropic liquid–cooling cycles can be performed before crystallisation occurs.

Obviously, the mesogenic behaviour of these complexes is driven by the *ortho*-metallated imine fragment, but the nature of the *N*-benzoylthiourea derivative, in particular R_1 and R_2 substituents, has a major influence on their mesogenic properties. It is important to note that, when compared to previously reported palladium(II) complexes bearing 4-hexyloxy benzylidene-4′-hexyloxyaniline as imine ligand and *N*-benzoyl thiourea derivatives as co-ligands, which exhibited only a strong monotropic nematic phase (*8*), the introduction of an additional alkoxy chain on the benzylidene ring together with longer carbon chains are responsible for the stabilisation of the lamellar phase. Thus, in the case of Pd(II) complexes bearing *N,N*-dialkyl-*N*′-benzoylthiourea derivatives (**3**–**7**), the melting points and the temperature of the transition from isotropic to SmA phase are influenced by the chain length (see Figure 4); there is a clear tendency of decrease of the stability of the SmA phase with the increasing the chain length up to butyl groups, followed by an increase when hexyl groups are replaced with octyl groups. An explanation for such behaviour could be discussed in terms of molecular anisotropy of these complexes, e.g. the length-to-breadth ratio (*19*). The terminal alkoxy chains on the imine fragment are unchanged, which means that

Table 1. Thermal data for palladium(II) and platinum(II) complexes.

Compound	M	Transition	T/°C	ΔH /kJ mol^{-1}
2		Cr–I	110	64.8
		(I–SmA)	(75)	(4.3)
3		Cr–Cr′	53	
		Cr′–I	62	60.6
		(I–SmA)	(53)	(2.9)
4		Cr–I	63	58.0
		(I–SmA)	(51)	(2.3)
5		Cr–Cr′	63	
		Cr′–I	71	49.6
		(I–N)	(44)	(0.7)
		(N–SmA)	(42)	(0.7)
6		Cr–I	68	38.7
		(I–N)	(55)	(0.9)
		(N–SmA)	(43)	(0.2)
7		Cr–Cr′	53	
		Cr′–I	62	25.5
		(I–SmA)	(52)	(2.8)
8	Pd	Cr–Cr′	43	3.0
		Cr′–I	71	57.0
		(I–SmA)	(26)	(2.3)
9		Cr–Cr′	59	43.2
		Cr′–I	80	24.3
		(I–SmA)	(58)	(4.3)
10		Cr–Cr′	67	58.5
		Cr′–I	85	8.7
		(I–SmA)	(53)	(3.7)
11		Cr–Cr′	66	13.8
		Cr′–I	91	31
		(I–SmA)	(55)	(3.3)
12		Cr–Cr′	71	24.7
		Cr′–I	93	29.8
		(I–SmA)	(56)	(3.1)
13	Pt	Cr–Cr′	67	53.7
		Cr′–I	73	
		(I–SmA)	(63)	(2.9)
14		Cr–I	79	35.9
		(I–SmA)	(70)	(4.2)

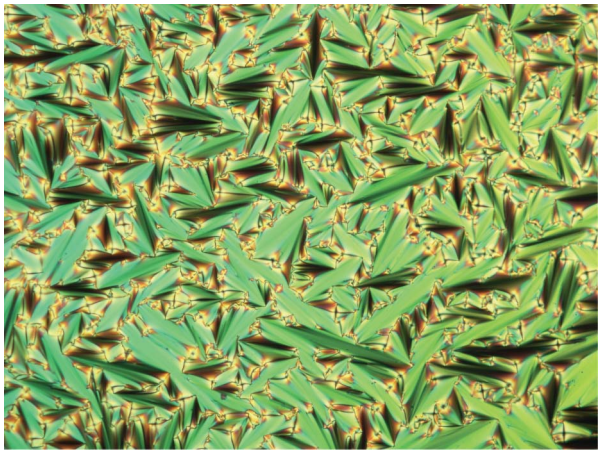

Figure 1. Polarising optical microphotograph of the SmA phase of compound **3** at 49°C (200×).

increasing the length of the alkyl chains of *N*-benzoylthiourea derivatives leads to the increase of the molecular breadth with immediate consequences on mesogenic behaviour. In this way, the minimum stability of the SmA phase is reached for complexes **5** and **6** when a short-range nematic phase appears. Further, as the alkyl chain becomes longer on going from butyl to octyl, we can assume that these chains adopt the conformation that runs along the mesogenic core and no further significant change in the stability of the SmA phase is seen. The same influence on transition temperatures with increasing the alkyl chain length from ethyl to octyl was observed for other *ortho*-metallated palladium(II) complexes bearing imine ligands and dialkyldithiocarbamates as co-ligands (*7*).

On the other hand, if we consider now the remainder of the materials, the Pd(II) complexes with *N*-benzoyl-*N*′-phenylthiourea derivatives (**8**–**12**), the complex **8** could be a useful starting point, based on an unsubstituted *N*-benzoyl-*N*′-phenyl ligand. This complex exhibits a low melting point, 71°C, and a strong monotropic SmA phase stable at room temperature with the lowest transition temperature from isotropic to SmA phase of all complexes. One reason for this behaviour could be the high flexibility of the structure adopted by this type of ligand with a less favourable molecular shape together with the intramolecular hydrogen bonds, N–H···S, that could be formed between the S atom of the thiocarbonyl group and the hydrogen atom of the amino –NHR group of the *N*-benzoylthiourea ligand. Thus, several new *N*-benzoylthiourea derivatives were introduced with the aim of establishing some structure–property correlations. It was found that, whereas the melting points were higher by 10–30°C when compared to their related complexes having *N*-dialkyl-*N*′-benzoylthiourea derivatives, the stability of SmA mesophase increased with increasing the size of the group attached to the benzene ring of BTU derivative, on going from F to Br and then to methoxy group. This tendency originates from the favourable lamellar packing as a consequence of the polarity of the lateral substituent located on the *N*-benzoylthiourea coligand combined with a space-filling effect. The most dramatic change occurs with the introduction of fluorine substituent in complex **9**, when the temperature of the transition from isotropic liquid to SmA was 32°C higher than the one of complex **8**. This could be readily explained by the introduction of a lateral dipole, which is responsible for the stabilisation of the lamellar packing. Now, a comparison of the mesogenic behaviour of the palladium and platinum complexes, which possess the same structure, reveals the same type of mesophases but with higher transition temperatures in the case of platinum complexes, which is a consequence of

Downloaded At: 14:54 25 January 2011

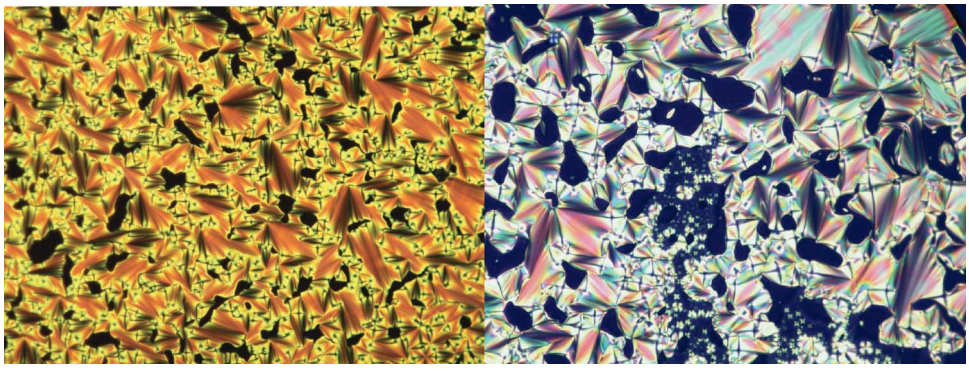

(a) (b)

Figure 2. Polarising optical microphotograph of the SmA phase of (a) compound **13** at 61°C and (b) **14** at 69°C (200×).

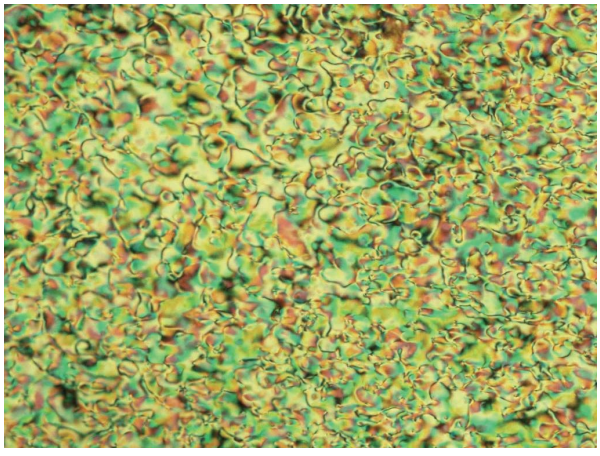

(a)

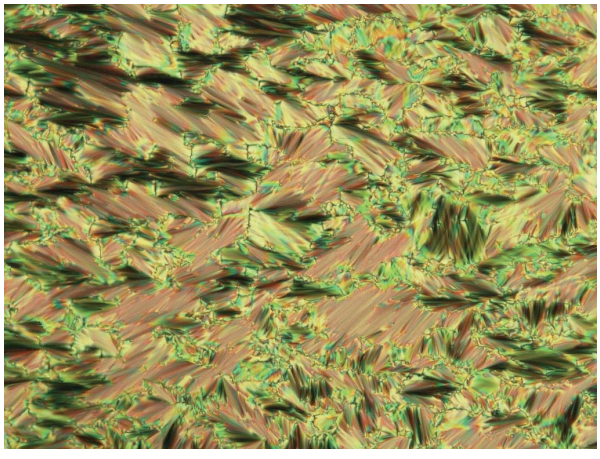

(b)

Figure 3. Polarising optical microphotographs of compound **5**, as observed on cooling: (a) nematic phase at 43°C; (b) SmA phase at 41°C (200×).

replacing palladium with the heavier platinum metal that brings an enhancement in polarisation. The stability of the smectic phase increased for both platinum(II) complexes, **13** and **14** compare to their Pd analogues (Figure 4). A similar change in mesogenic properties, when replacing palladium with platinum, was reported for other *ortho*-metallated imine complexes (*20*).

2.2 *TSDC measurements*

The experimental set-up for TSDC measurements has been described in detail elsewhere (*21, 22*). Figure 5 shows the heating–cooling steps of the experiment. In the first heating step (0), from room temperature to a

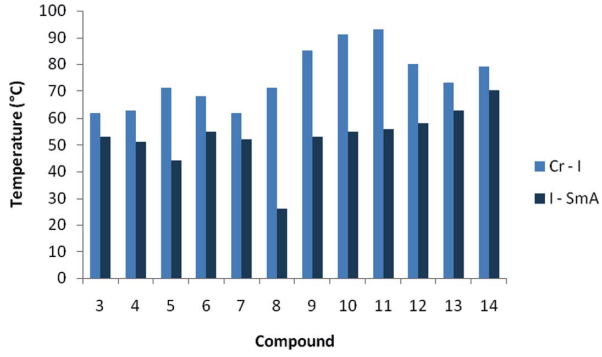

Figure 4. Thermotropic behaviour of Pd(II) and Pt(II) complexes ($T_{I\text{-}N}$ is included for complexes **5** and **6**).

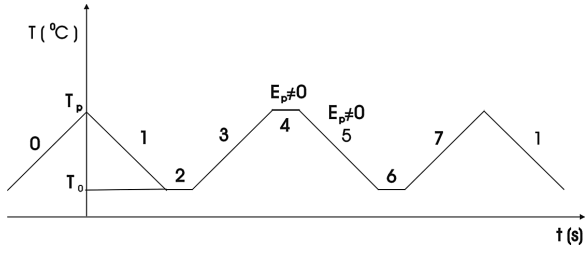

Figure 5. Heating–cooling cycles applied to the sample.

Downloaded At: 14:54 25 January 2011

pre-established temperature (T_p), higher than the smectic to isotropic transition temperature of the liquid crystal, initial depolarisation of the sample takes place. During the steps 1, 2, and 3 the polarising field $E_p = 0$; these steps are performed to eliminate the eventuality of charges existing due to previously treatments applied to the sample (manufacturing or previously applied heating–cooling cycles and electric field).

During step 4, at T_p, the polarising field $E_p = V_p/g$ is applied (V_p is the voltage applied to the sample and g is the thickness of the sample) and it is maintained during the cooling down to T_0 (step 5). During the step 6, the field E_p is cut off and the sample is short-circuited to eliminate capacitive discharge. The depolarising currents are registered during step 7. The heating–cooling rates were 1 K min^{-1} and steps 2, 4 and 6 were 15 min in duration. In this experiment, the polarisation temperature is $T_p = 80°C$ and $T_0 = 25°C$.

The optical beam from a light source is transmitted through the sample and measured by the photomultiplier; crossed polarisers have been used.

According to the heating–cooling cycles presented in Figure 5, the electrical field E_p is applied to the sample at the higher temperature T_p and it is maintained constant during cooling. The polarisation of the dielectrics submitted to an external electric field is due to the mechanisms involving microscopic or macroscopic charge displacement. Since the internal friction and ionic mobility depend exponentially on temperature, heating a dielectric to a high temperature T_p enhances the response time of permanent dipoles and internal free charges to the applied electric field and allows the equilibrium polarisation to be reached in short time. When the polarisation field is maintained while cooling the sample to a temperature T_o sufficiently low to increase the relaxation times of the dipoles and ions to values of hours or more, these are practically "frozen" in the electrical configuration reached at T_p and consequently do not respond when the field is switched off. The equilibrium polarisation $P_e(T_p)$ reached during the polarisation phase 5 is consequently considered constant at the end of the cooling, when the heating step begins (step 7).

In step 7, the thermally induced depolarisation currents are measured. The thermally stimulated depolarisation currents versus temperature are shown in Figure 6. It can be seen that at the smectic–isotropic phase transition the current has a minimum, the value of which increases with the polarising voltage.

Consider that the charge given by (*23, 24*):

$$Q = -\int_{t_1}^{t_2} i(t)dt = -\frac{dt}{dT}\int_{T_1}^{T_2} i(T)dT, \qquad (1)$$

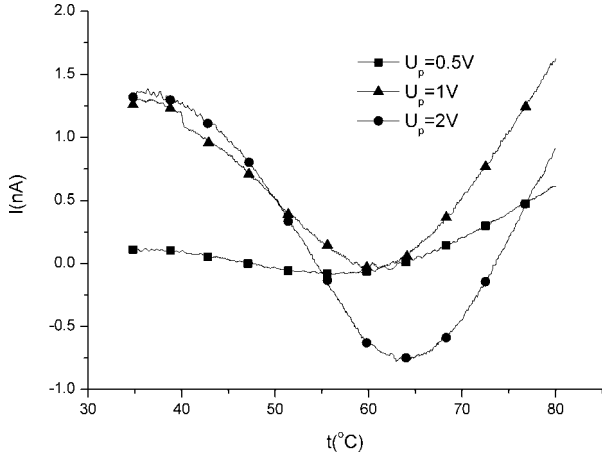

Figure 6. TSDC spectra for complex **3**, step 7, after applying different polarisation voltages in previous step 5.

where t_1 and t_2 represent the times between which the temperature varies from T_1 to T_2 with a linear constant rate. We notice that the sign of the charge depends on the sign of the current and on the sign of variation with temperature, $\frac{dt}{dT}$; for step 7, the last term is positive, because the temperature is increasing.

Considering the polarity of the voltage applied on the sample positive compared to the ground, it follows that if the current is positive, it is produced by a heterocharge (with a polarity opposing that of the electrode), and if the current is negative, it is due to a homocharge. In our experiments, the TSDC diagrams have shown negative currents, due to homocharges (*25*).

The Arrhenius curve corresponding to a decrease of the temperature, at 0.5 V, is depicted in Figure 7. As can be seen from the graph, this slope exhibits a discontinuity at approximate 53.7°C. When measured at 0.5 V, the activation energy is 0.958 eV for

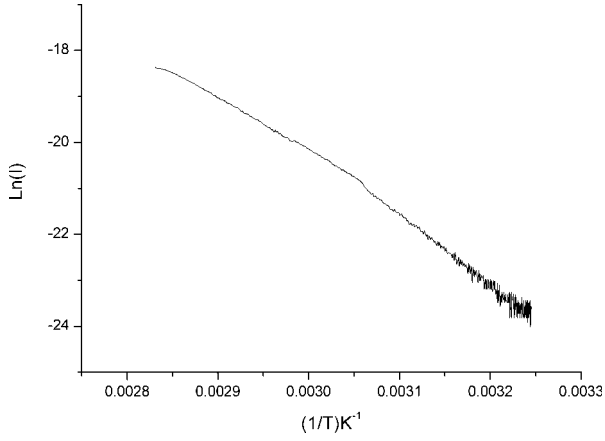

Figure 7. Arrhenius curve, $\ln(I) = f(1/T)$, step 5, at the decrease of the temperature, at 0.5 V polarisation voltage.

Downloaded At: 14:54 25 January 2011

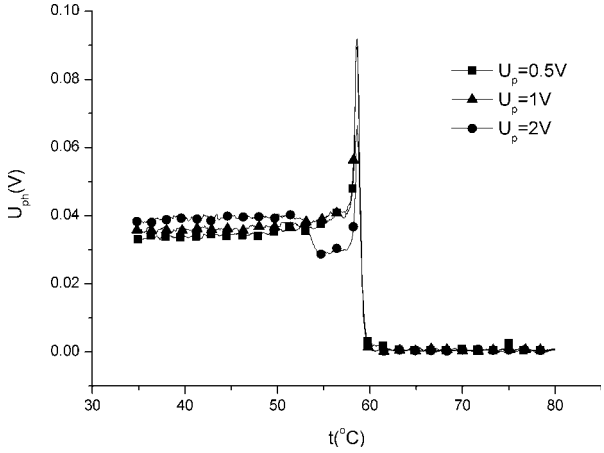

Figure 8. Optical transmission versus temperature, measured for complex **3** in step 7, after different polarisation voltages applied in step 5.

temperatures higher than 62°C and 1.32 eV for temperatures lower than 55°C. For a voltage of 1 V, the activation energy becomes 0.968 eV above 62°C and 1.23 eV below 55°C. It follows that the difference between the activation energies in the specified domains decreases with the polarising voltage, which can be assigned to the freezing of the structure with the electric field.

Figure 8 shows the optical transmission measured with increasing of the temperature, after applying different polarisation voltages to the sample. The following observations can be made.

(1) The optical transmission has a sharp maximum at the SmA–I phase transition temperature. This might be explained by the presence of the SmA–I phase transition frontier. This region is strongly birefringent and might determine an increase of the optical signal while it is present in the optical field of the microscope. The temperature of SmA–I transition was recorded during the heating cycle, step 7; it is important to note here that this compound, on cooling, remains in the SmA phase at room temperature.
(2) With a further increase of the temperature, to the isotropic phase, the transmission decreases.
(3) The optical transmission depends slightly with the polarising voltage applied in step 5, explained by the partial "freezing" of the crystal structure.

3. Conclusions

A series of *ortho*-metallated Pd and Pt complexes containing an imine ligand carrying three alkoxy chains and *N*-benzoylthiourea derivatives as co-ligands have been synthesised and their liquid crystalline properties investigated. All the compounds exhibit monotropic transitions with nematic and SmA phases being displayed, with the mesomorphic behaviour strongly related to the type of *N*-benzoylthiourea ligand as well as the metal centre used. The TSDC technique was employed to determine the conduction mechanism, phase transition temperature and the activation energies for an organometallic palladium(II) compound that contains an *ortho*-metallated imine fragment. The influence of previously applied electric fields on the phase transition temperature was studied. The SmA–I transition temperature increases with an increase of the pre-applied voltage. The optical transmission in the smectic state increases slightly with a previously applied electric field.

4. Experimental

Dichloromethane was distilled from phosphorus pentaoxide; other chemicals were used as supplied.

^{1}H NMR spectra were recorded on a Varian Gemini 300 BB spectrometer operating at 300 MHz, using $CDCl_3$ as solvent. ^{1}H chemical shifts were referenced to the solvent peak position, δ7.26. Analysis by DSC was carried out with Perkin-Elmer DSC7 and Diamond instruments using 5 and 10°C min^{-1} scanning rates. Two or more heating–cooling cycles were performed on each sample. Mesomorphism was studied by hot-stage POM using a Nikon 50i Pol microscope equipped with a Linkam THMS600 hot stage and a TMS94 temperature controller. Mesophases were assigned by their optical texture (*26*). For sample preparation for TSDC measurements, the liquid crystalline compound **3** was filled in an 18 μm thick ITO-covered sandwich-type glass cell.

The *N*-benzoylthiourea derivatives and their sodium salts used in this work were prepared according to methods published in the literature (*27*).

4.1 Synthesis of imine ligand 1

To a solution of p-decyloxyaniline (0.249 g, 1 mmol) in ethanol (20 cm^3), 3,4-didecyloxybenzaldehyde (0.418 g, 1 mmol) followed by five drops of glacial acetic acid were added. The mixture was heated under reflux for 2 h and then cooled to –25°C to give the crude product. Recrystallisation from hot ethanol gave the analytically pure product as off-white crystals.

4.2 Synthesis of dinuclear palladium(II) and platinum(II) complexes

The imine ligand (2.5 mmol) was dissolved in dichloromethane (30 cm^3) and palladium acetate trimer

Downloaded At: 14:54 25 January 2011

(0.83 mmol) was added. The resulting mixture was stirred at room temperature for 18 h after which the solvent was removed in vacuo. The residue was crystallised from a mixture dichloromethane–ethanol to give the yellow-green crystalline products, which were washed with cold ethanol and dried under vacuum.

In the case of chloro-bridged dinuclear platinum(II) complexes, the starting material was $[Pt(\mu\text{-}Cl)(\eta^3\text{-}C_4H_7)]_2$, which was prepared according to literature data (*28*). Thus, the mixture of the imine ligand and $[Pt(\mu\text{-}Cl)(\eta^3\text{-}C_4H_7)]_2$ in methanol, in molar ratio 2:1, was stirred for 1 day at room temperature. The resulting brown precipitate was filtered and washed several times with cold methanol. The preparation of the dinuclear platinum(II) complexes followed the procedure described in the literature (*29*). The crude product was used in the next step, for the preparation of mononuclear species, without further purification.

4.3 Synthesis of mononuclear palladium(II) and platinum(II) complexes 3–14

The synthesis of **3** is described here. The other Pd(II) and Pt(II) complexes were prepared in the same manner using binuclear palladium or platinum complex/sodium salt of *N*-benzoylthiourea with a molar ratio of 1:3.

Solid sodium salt of *N*,*N*-diethyl-*N*′-benzoylthiourea (0.0715 g, 0.27 mmol) was added to a solution of binuclear palladium complex (0.075 g, 0.09 mmol) in dichloromethane (15 cm^3) and the mixture stirred at room temperature for 24 h. Evaporation of the solvent gave a yellow solid, which was purified by chromatography on silica using dichloromethane as eluent to give a yellow solid. This was recrystallised from a mixture of dichloromethane/ethanol (1/1) at –25°C.

The platinum(II) complexes were recrystallised from a mixture of acetone/methanol (1/1) at –25°C.

The yields, elemental analysis results as well as ^1H NMR data are presented below.

For complex **1**: yield 47%, as off-white crystals; m.p. 74°C. Elemental analysis: calculated for $C_{43}H_{71}NO_3$, C 79.5, H 11.0, N 2.2; found, C 79.1, H 11.4, N 2.4%. ^1H NMR (300 MHz, $CDCl_3$): 8.35 (s, 1H, CH=N), 7.60 (d, broad, 1H), 7.27 (dd, J = 1.8 Hz and J = 8.3 Hz, 1H), 7.19 (AA′BB′ system, J = 8.9 Hz, 2H aniline ring), 6.92 (d, J = 8.9 Hz, 3H), 4.12–4.03 (m, 4H, $2OCH_2$ groups), 3.97 (t, J = 6.5 Hz, 2H, OCH_2), 1.90–1.25 (m, 40H, CH_2 groups), 0.95–0.85 (m, 9H, CH_3 groups). IR (cm^{-1}): 1621 ($\nu_{C=N}$), 1266, 1243 ($\nu_{C\text{-}O\text{-}C}$).

For complex **2**: yield 63%, as yellow crystals. Elemental analysis: calculated for $C_{90}H_{146}N_2O_{10}Pd_2$, C 66.4, H 9.0, N 1.7; found, C 63.9, H 9.4, N 1.5%. ^1H NMR (300 MHz, $CDCl_3$): 7.43 (s, 1H), 6.81 (s, 1H), 6.65 (q, J = 7.0 Hz, 4H), 5.99 (s, 1H), 3.99–3.45 (m, 6H), 1.89 (s, 3H), 1.78 (m, 6H), 1.52–1.24 (m, 26H), 0.95–0.85 (m, 9H). IR (cm^{-1}): 1597 ($\nu_{C=N}$), 1259 ($\nu_{C\text{-}O\text{-}C}$).

For complex **3**: yield 72%. Elemental analysis: calculated for $C_{55}H_{85}N_3O_4PdS$(%), C 66.7, H 8.6, N 4.2; found, C 66.3, H 9.1, N 4.7%. ^1H NMR ($CDCl_3$, 300 MHz): 8.08 (1H, s), 7.76 (2H, m), 7.40–7.35 (3H, m), 7.24–7.21 (2H, m), 7.01–6.95 (4H, m), 4.17–3.83 (10H, m), 1.90–1.20 (48H, m), 0.88 (15H, m). IR (cm^{-1}): 1588($\nu_{C=N}$), 1528(δ_{NH}), 1418(ν_{CN+CS}).

For complex **4**: yield 75%. Elemental analysis: calculated for $C_{57}H_{89}N_3O_4PdS$(%), C 67.2, H 8.8, N 4.1; found, C 66.9, H 9.2, N 3.8%. ^1H NMR ($CDCl_3$, 300 MHz): 8.08 (1H, s), 7.77 (2H, m), 7.40–7.33 (3H, m), 7.22 (2H, m), 7.01 (2H, s br), 6.97 (2H, d, AA′XX′, J = 8.8 Hz), 4.14 (2H, t, J = 6.8 Hz), 4.02 (2H, t, J = 6.5 Hz), 3.94 (2H, t, J = 6.7 Hz), 3.89–3.75 (4H, m), 1.96–1.20 (52H, m), 1.03 (3H, t, J = 7.4 Hz), 0.97–0.85 (12H, m). IR (cm^{-1}): 1584($\nu_{C=N}$), 1515(δ_{NH}), 1420(ν_{CN+CS}).

For complex **5**: yield 68%. Elemental analysis: calculated for $C_{59}H_{93}N_3O_4PdS$(%), C 67.7, H 9.0, N 4.0; found, C 67.5, H 9.4, N 3.85. ^1H NMR ($CDCl_3$, 300 MHz): 8.08 (1H, s), 7.77 (2H, m), 7.41–7.34 (3H, m), 7.27–7.19 (2H, m), 7.01 (1H, s), 7.00 (1H, s), 6.97 (2H, d, AA′XX′, J = 8.9 Hz), 4.11 (2H, t, J = 6.7 Hz), 4.02 (2H, t, J = 6.5 Hz), 3.96–3.78 (6H, m), 1.94–1.23 (56H, m), 1.05 (3H, t, J = 7.3 Hz), 0.95–0.85 (12H, m). IR (cm^{-1}): 1585($\nu_{C=N}$), 1523(δ_{NH}), 1418(ν_{CN+CS}).

For complex **6**: yield 81%. Elemental analysis: calculated for $C_{63}H_{101}N_3O_4PdS$(%), C 68.6, H 9.2, N 3.8; found, C 68.3, H 9.6, N 3.5%. ^1H NMR ($CDCl_3$, 300 MHz): 8.08 (1H, s), 7.77 (2H, m), 7.43–7.34 (3H, m), 7.22 (2H, m), 7.01 (1H, s), 7.00 (1H, s), 6.97 (2H, d, AA′XX′, J = 8.9 Hz), 4.13 (2H, t, J = 6.6 Hz), 4.02 (2H, t, J = 6.5 Hz), 3.97 – 3.75 (6H, m), 1.90–1.25 (64H, m), 0.95–0.85 (15H, m). IR (cm^{-1}): 1586($\nu_{C=N}$), 1523(δ_{NH}), 1423(ν_{CN+CS}).

For complex **7**: yield 65%. Elemental analysis: calculated for $C_{67}H_{109}N_3O_4PdS$(%), C 69.4, H 9.5, N 3.6; found, C 68.9, H 9.9, N 3.3%. ^1H NMR ($CDCl_3$, 300 MHz): 8.08 (1H, s), 7.78 (2H, m), 7.41–7.34 (3H, m), 7.22 (2H, m), 7.01 (2H, s br), 6.97 (2H, d, AA′XX′, J = 8.8 Hz), 4.14 (2H, t, J = 6.6 Hz), 4.02 (2H, t, J = 6.5 Hz), 3.97–3.75 (6H, m), 1.90–1.25 (64H, m), 0.95–0.85 (15H, m). IR (cm^{-1}): 1585($\nu_{C=N}$), 1522(δ_{NH}), 1418(ν_{CN+CS}).

For complex **8**: yield 62%. Elemental analysis: calculated for $C_{57}H_{81}N_3O_4PdS$(%), C 67.7, H 8.1, N 4.2; found, C 67.4, H 8.5, N 3.8%. ^1H NMR ($CDCl_3$, 300 MHz): 8.08 (1H, s), 7.75 (2H, m), 7.62–7.57 (2H, m), 7.41–7.35 (6H, m), 7.23–7.17 (2H, m), 7.02 (1H, s),

Downloaded At: 14:54 25 January 2011

6.98 (2H, d, AA′XX′, J = 8.9 Hz), 6.86 (1H, s), 4.12 (2H, m), 4.03 (2H, t, J = 6.5 Hz), 3.95 (2H, t, J = 6.7 Hz), 1.90–1.25 (42H, m), 0.89 (15H, m). IR (cm^{-1}): 1591($\nu_{C=N}$), 1534(δ_{NH}), 1417(ν_{CN+CS}).

For complex **9**: yield 70%. Elemental analysis: calculated for $C_{58}H_{83}N_3O_5PdS$(%), C 66.9, H 8.0, N 4.0; found, C 66.8, H 8.2, N 3.8%. ^{1}H NMR ($CDCl_3$, 300 MHz): 8.07 (1H, s), 7.96 (2H, m), 7.71 (2H, m), 7.46 (2H, d, AA′XX′, J = 8.9 Hz), 7.38 (2H, d, AA′XX′, J = 8.9 Hz), 7.24–7.17 (2H, m), 7.01 (1H, s), 6.97 (2H, d, AA′XX′, J = 8.9 Hz), 6.93–6.85 (2H, m), 4.12 (2H, m), 4.02 (2H, t, J = 6.5 Hz), 3.92 (2H, t, J = 6.6 Hz), 3.83 (s, 3H), 1.88–1.23 (42H, m), 0.87 (15H, m). IR (cm^{-1}): 1581($\nu_{C=N}$), 1536(δ_{NH}), 1430(ν_{CN+CS}).

For complex **10**: yield 67%. Elemental analysis: calculated for $C_{57}H_{80}FN_3O_4PdS$(%), C 66.5, H 7.8, N 4.1; found, C 66.4, H 8.0, N 3.95. ^{1}H NMR ($CDCl_3$, 300 MHz): 8.07 (1H, s), 7.71 (2H, m), 7.54–7.48 (2H, m), 7.40–7.36 (3H, m), 7.22 (2H, t br), 7.07 (2H, t, AA′MXX′, J = 8.6 Hz), 7.01 (1H, s), 6.97 (2H, d, AA′XX′, J = 8.8 Hz), 6.85 (1H, s br), 4.11 (2H, m), 4.02 (2H, t, J = 6.6 Hz), 3.94 (2H, t, J = 6.7 Hz), 1.90–1.25 (42H, m), 0.89 (15H, m). IR (cm^{-1}): 1586($\nu_{C=N}$), 1536(δ_{NH}), 1427(ν_{CN+CS}).

For complex **11**: yield 73%. Elemental analysis: calculated for $C_{57}H_{80}ClN_3O_4PdS$(%), C 65.5, H 7.7, N 4.0; found, C 65.0, H 8.2, N 3.85. ^{1}H NMR ($CDCl_3$, 300 MHz): 8.07 (1H, s), 7.73 (2H, m), 7.53 (2H, d, AA′XX′, J = 8.9 Hz)), 7.42–7.36 (3H, m), 7.33 (2H, d, AA′XX′, J = 8.9 Hz), 7.25 (2H, m), 7.01 (1H, s), 6.98 (2H, d, AA′XX′, J = 8.9 Hz), 6.84 (1H, s br), 4.12 (2H, m), 4.02 (2H, t, J = 6.5 Hz), 3.94 (2H, t, J = 6.6 Hz), 1.90–1.25 (42H, m), 0.88 (15H, m). IR (cm^{-1}): 1589($\nu_{C=N}$), 1535(δ_{NH}), 1426(ν_{CN+CS}).

For complex **12**: yield 64%. Elemental analysis: calculated for $C_{57}H_{80}BrN_3O_4PdS$(%), C 62.8, H 7.4, N 3.9; found, C 62.5, H 7.8, N 3.55. ^{1}H NMR ($CDCl_3$, 300 MHz): 8.07 (1H, s), 7.72 (2H, m), 7.48 (4H, s br), 7.43–7.36 (3H, m), 7.25 (2H, m), 7.01 (1H, s), 6.98 (2H, d, AA′XX′, J = 8.9 Hz), 6.83 (1H, s br), 4.12 (2H, m), 4.03 (2H, t, J = 6.6 Hz), 3.94 (2H, t, J = 6.7 Hz), 1.989–1.26 (42H, m), 0.90 (15H, m). IR (cm^{-1}): 1589($\nu_{C=N}$), 1535(δ_{NH}), 1425(ν_{CN+CS}).

For complex **13**: yield 27%. Elemental analysis: calculated for $C_{57}H_{89}N_3O_4PtS$(%), C 61.8, H 8.1, N 3.8; found, C 61.5, H 8.5, N 3.6%. ^{1}H NMR ($CDCl_3$, 300 MHz): 8.33 (1H, s, $J_{Pt\text{-}H}$ = 115 Hz), 7.68 (2H, m), 7.40–7.35 (3H, m), 7.26–7.15 (2H, m), 7.05 (1H, s), 7.03 (1H, s), 6.97 (2H, d, AA′XX′, J = 8.9 Hz), 4.11 (2H, t, J = 6.9 Hz), 4.03 (2H, t, J = 6.5 Hz), 3.93 (2H, t, J = 6.7 Hz), 3.89–3.75 (4H, m), 1.90–1.25 (52H, m), 1.05 (3H, t, J = 7.3 Hz), 0.95–0.85 (12H, m). IR (cm^{-1}): 1589($\nu_{C=N}$), 1514(δ_{NH}), 1417(ν_{CN+CS}).

For complex **14**: yield 32%. Elemental analysis: calculated for $C_{67}H_{109}N_3O_4PtS$(%), C 64.5, H 8.8, N 3.4; found, C 64.1, H 9.3, N 3.1%. ^{1}H NMR ($CDCl_3$, 300 MHz): 8.33 (1H, s, $J_{Pt\text{-}H}$ = 114 Hz), 7.67 (2H, m), 7.42–7.35 (3H, m), 7.19 (2H, m), 7.05 (1H, s), 7.02 (1H, s), 6.96 (2H, d, AA′XX′, J = 8.8 Hz), 4.13 (2H, t, J = 6.6 Hz), 4.03 (2H, t, J = 6.4 Hz), 3.93 (2H, t, J = 6.4 Hz), 3.86–3.73 (4H, m), 1.85–1.15 (64H, m), 0.92–0.82 (15H, m). IR (cm^{-1}): 1587($\nu_{C=N}$), 151(δ_{NH}), 1417(ν_{CN+CS}).

Aknowledgements

The authors wish to thank MEdC (Romanian Ministry of Education and Research, project CNCSIS-1640, project PNII ID_954 and project PNII ID_123) and NATO for funding this study and to Prof. Duncan W. Bruce (University of York, UK) for his support.

References

(1) Donnio, B.; Guillon, D.; Deschenaux, R.; Bruce D.W. In *Comprehensive Coordination Chemistry II;* McCleverty, J.A., Meyer, T.J., Eds.; Elsevier: Oxford, 2003; Volume 7, Chapter 7.9, pp 357–627; Serrano, J.-L., Ed. *Metallomesogens;* Wiley-VCH: Weinheim, 1996.

(2) Donnio, B.; Guillon, D.; Deschenaux, R.; Bruce, D.W. in *Comprehensive Organometallic Chemistry III;* Crabtree, R.H., Mingos D.M.P., Eds.; Elsevier: Oxford, 2006; Volume 12, Chapter 12.05, pp 195–293; Donnio, B.; Bruce, D.W. in *Palladacycles;* Dupont, J., Pfeffer, M., Eds.; Wiley-VCH: Weinheim, 2008.

(3) (a) Buey, J.; Espinet, P. *J. Organomet. Chem.* **1996,** *507,* 137–145; (b) Baena, M.J.; Espinet, P.; Ros, M.B.; Serrano, J.L. *Angew. Chem., Int. Ed.* **1991,** *30,* 711–712. (c) Omnès, L.; Timimi, B.A.; Gelbrich, T.; Hursthouse, M.B.; Luckhurst, G.R.; Bruce, D.W. *Chem. Commun.* **2001,** 2248–2249; (d) Cave, G.W.V.; Lydon, D.P.; Rourke, J.P. *J.Organomet. Chem.* **1998,** *555,* 81–88; (e) Cîrcu, V.; Gibbs, T.J.K.; Omnès, L.; Horton, P.N.; Hursthouse, M.B.; Bruce., D.W. *J. Mater. Chem.* **2006,** *16,* 4316–4325.

(4) Buey, J.; Espinet, P.; Kitzerow, H.S.; Strauss, J. *Chem. Commun.* **1999,** 441–442.

(5) (a) Huang, D.J.; Xiong, N.Y.; Yang, J.; Wang, S.M.; Li, G.N.; Zhang, L.F. *Mol. Cryst. Liq. Cryst.* **1993,** *231,* 191–198; (b) Saccomando, D.J.; Black, C.; Cave, G.W.V.; Lydon, D.P.; Rourke, J.P. *J. Organomet. Chem.* **2000,** *601,* 305–310.

(6) Lydon, D.P.; Cave, G.W.V.; Rourke, J.P. *J. Mater. Chem.* **1997**, *7*, 403–406.

(7) Diez, L.; Espinet, P.; Miguel, J.A. *J. Chem. Soc., Dalton Trans.* **2001**, 1189–1195.

(8) Tenchiu, A.C.; Iliş, M.; Dumitraşcu, F.; Whitwood, A.C.; Cîrcu, V. *Polyhedron* **2008**, *27*, 3537–3544.

(9) 9. (a) Beyer, L.; Hoyer, E.; Liebscher, J.; Hartmann, H. *Z. Chem.* **1981,** *21,* 81–91; (b) Muhl, P.; Gloe, K.; Dietze, F.; Hoyer, E.; Beyer, L. *Z. Chem.* **1986,** *26,* 81–94; (c) Koch, K.R. *Coord. Chem. Rev.* **2001,** *216–217,* 473–488.

(10) Seshadri, T.; Haupt, H.-J. *J. Mater. Chem.* **1998**, *8*, 1345–1350.

Downloaded At: 14:54 25 January 2011

(11) Deleanu, A.; Ilis, M.; Rosu, T.; Cîrcu, V. *Rev. Chim. (Bucharest)* **2006**, *57*, 1216–1220.
(12) Seshadri, T.; Haupt, H.-J.; Flörke, U.; Henkel, G. *Liq. Cryst.* **2007**, *34*, 33–47.
(13) Bilgin-Eran, B.; Tschierske, C.; Diele, S.; Baumeister, U. *J. Mater. Chem.* **2006**, *16*, 1136–1144.
(14) Bilgin-Eran, B.; Singer, D.; Praefcke, K. *Eur. J. Inorg. Chem.* **2001**, 111–116.
(15) Vanderscueren, J.; Gassiot, J. in *Thermally Stimulated Relaxation in Solids;* Braunlich, P., Springer–Verlag: Berlin,1979.
(16) van Turnhout, J. *Thermally Stimulated Discharge of Polymer Electrets*; Elsevier: Amsterdam, 1975; pp 104–108.
(17) (a) Pregosin, P.S.; Wombacher, F.; Albinati, A.; Lianza, F. *J. Organomet. Chem.* **1991,** *418,* 249–267; (b) Cîrcu, V.; Horton, P.N.; Hursthouse, M.B.; Bruce, D.W. *Liq. Cryst*. **2007,** *34,* 1463–1472.
(18) Bilgin-Eran, B.; Tschierske, C.; Diele, S.; Baumeister, U. *J. Mater. Chem.* **2006**, *16*, 1145–1153.
(19) Collings, P.J.; Hird, M. *Introduction to Liquid Crystals Chemistry and Physics*; Taylor & Francis: London, 2004.
(20) (a) Ortega, J.; Folcia, C.L.; Etxebarria, J.; Ros, M.B.; Miguel, J.A. *Liq. Cryst.* **1997,** *23,* 285–291; (b) Diez, L.; Espinet, P.; Miguel, J.A.; Ros, M.B. *J. Mater. Chem.* **2002,** *12,* 3694–3698.
(21) Roşu, C.; Mănăilă-Maximean, D.; Godinho, M.H.; Almeida, P.L. *Mol. Cryst. Liq. Cryst*. **2003**, *391*, 1–11.
(22) Roşu, C.; Mănăilă-Maximean, D.; Paraskos, A. *Mod. Phys. Lett. B* **2002**, *16*, 317–352.
(23) Jackson, J.D. *Classical Electrodynamics*; John Wiley & Sons: New York, 1991.
(24) Seanor, D.A. *Adv. Polym. Sci*. **1965**, *4*, 317–352.
(25) Frölich, H. *Theory of Dielectrics*; Clarendon Press: Oxford, 1949.
(26) Dierking, I. *Textures of Liquid Crystals*; Wiley-VCH Verlag: Weinham, 2003.
(27) Douglass, I.B.; Dains, F.B. *J. Am. Chem. Soc.* **1934**, *56*, 719–721.
(28) Mabbot, D.J.; Mann, B.E.; Maitlis, P.M. *J. Chem. Soc., Dalton Trans.* **1977**, 294–299.
(29) Buey, J.; Diez, L.; Espinet, P.; Kitzerow, H.-S.; Miguel, J.A. *Chem. Mater.* **1996**, *8*, 2375–2381.

Downloaded At: 14:54 25 January 2011